Structural behaviour of RC beams externally strengthened with FRP sheets under fatigue and monotonic loading

J.F. Dong [a,b], Q.Y. Wang [a,*], Z.W. Guan [b]

[a] School of Architecture and Environment, Sichuan University, Chengdu 610065, PR China
[b] School of Engineering, University of Liverpool, Liverpool L69 3GH, United Kingdom

ARTICLE INFO

ABSTRACT

This paper presents experimental research on the fatigue and post-fatigue static behaviour of reinforced concrete beams strengthened with glass or carbon fibre reinforced polymer (FRP) sheets placed either vertically or obliquely. All beams for fatigue tests were subjected to four-point bending for one million cycles with a frequency of 5 Hz. The results show that the FRP sheets can be used to significantly enhance the fatigue resistance of the beams strengthened. Also the results from the post-fatigue monotonous tests indicate that FRP sheets contribute the significant increase of the ultimate strength and ductility of the beams tested. The diagonal GFRP reinforcing arrangement is more effective than the vertical one in enhancing shear strength and stiffness. Finally, some moment deflection models were adapted to predict the ultimate loads of the beams tested, which give very good correlation to the experimental results.

1. Introduction

In recent years, there are many reinforced concrete (RC) structures are suffering from various deteriorations: cracks, concrete spalling, large deflection, etc., which need to be reinforced to support the designed or even resist possible higher loading or to renovate existing cracks [1–3]. These deteriorations are caused by various factors such as aging, corrosion of steel reinforcement, environmental effects such as seawater and accidental impacts on the structure [4–6]. Especially, during the natural disasters such as the earthquake in Sichuan on 12th May, 2008, many concrete structures, if they were not collapsed, were damaged to some extent [7]. There are several options available for retrofitting or repairing structural members of the existing RC structures. The commonly used options are to bond thin steel and/or fibre reinforced polymer (FRP) sheets onto the damaged members to restrain cracks and to increase the load carrying capacity, ductility and stiffness of structures strengthened [8,9].

To externally bond FRP sheets on the tension and also lateral sides of RC beams and columns is a widely used method for repairing and strengthening of the RC structures. Such reinforcing technique is an effective way to improve the flexural and/or shear performance of the RC structures reinforced, since FRP has better characteristics than the conventional strengthening

material steel, in terms of high tensile strength, lightweight, resistance to corrosion and fatigue, etc. [3,5,10,11]. Investigations [12,13] were undertaken in the past to evaluate reliability of such reinforcing technique related to static loading and showed that the RC structures strengthened would demonstrate a better performance in strength, ductility and retarding crack growth as long as an appropriate end anchorage was provided for the FRP sheet [3,11].

More recently, through either experimental, the finite element or analytical approaches [14–19], extensive researches have been undertaken on behaviour of reinforced concrete beams strengthened by externally bonded FRP sheets for enhancing their flexural and shear performance. However, those studies primarily considered static behaviour of the FRP strengthened beams under monotonic loading. In fact, many structures such as bridges and marine structures are subjected to repeated cyclic loadings rather than static ones, and this is often overlooked in the analysis and design of RC beams strengthened with FRP sheets. It has been well established that externally bonding of the FRP on RC beams is an effective strengthening technique to increase their static strength and ductility, as well as fatigue resistance with high energy dissipation [20–25]. However, the scarcity of experimental data on fatigue behaviour of RC beams strengthened by the FRP sheet is unanimously recognized [26], which does not satisfy the design need. Therefore, to study fatigue performance of RC beams strengthened by the FRP sheets is necessary work to increase the knowledgebase in this area.

* Corresponding author. Tel./fax: +86 28 85406919.
E-mail address: wangqy@scu.edu.cn (Q.Y. Wang).

At the present, the main research work increasingly focuses on experimental flexural fatigue and shear fatigue. Nanni [27] showed that steel fibre reinforced concrete (SFRC) could enhance the fatigue performance and the fibre content was an effective parameter to influence the fatigue characteristics of beams tested. Chang and Chai [28] developed a test methodology to investigate the flexural fracture and fatigue of the SFRC beams. Leung et al. [29] studied the flexural fatigue performance of concrete beams using engineered cementitious composites (ECC) and found that the ECC could improve the fatigue life of the beam in controlling the growth of small cracks. Manfredi and Pecce [30] studied the failure modes and the relationship between the damage function and the cyclic degradations of the normal and high strength concrete beams under monotonic and cyclic loading. Research on concrete beams strengthened with carbon fibre reinforced polymer (CFRP) was carried out to investigate the influence of loading history on the fatigue life and crack width [31], and to analyze the relationship between the fatigue performance and the electrical property of CFRP under flexural loading [4]. Although a reasonable amount of research has been undertaken on the flexural fatigue [28–35], research on the shear fatigue performance of RC beams strengthened by CFRP and glass fibre reinforced polymer (GFRP) sheets however is limited up to date. Kwak and Kim [36] focused on the shear fatigue loading on the fatigue behaviour and strength of the polymer reinforced concrete (PRC) beams. Czaderski and Motavalli [24] studied RC beams strengthened by the CFRP L-shaped plates under shear fatigue loading. Moreover, some experimental research has also been conducted on the bonding behaviour between the FRP sheet and concrete under cyclic fatigue loading [10,17,20,21,26], since such the bonding behaviour influences the failure mode of the beam strengthened [34]. It was observed in these studies that if there was no obvious interfacial debonding between the FRP and concrete occurred fatigue behaviour of the FRP-strengthened beams would be improved. However, once debonding occurred, the deflection would be increased significantly and the tension cracks appeared near the position of the point loads applied [35]. Lu and Ayoub [37] studied the debonding failure on the response of RC beams and developed a new model to evaluate the reduction factor of FRP-strengthened RC beams due to FRP debonding. Yun et al. [38] demonstrated the effect of different bonding systems under fatigue loading on the long-term behaviour of the bond between the FRP and concrete. Carloni et al. [39] investigated the role of the FRP-concrete interface debonding under fatigue loading and found that debonding occurred during fatigue, which was related to the load range applied.

The work presented here aims research on the shear fatigue behaviour of RC beams made with the normal concrete strengthened with FRP (CFRP or GFRP) sheets. It is focused on investigating the effectiveness of FRP sheets on the fatigue behaviour and their contributions to the ultimate strength of ordinary RC beams. It also helps understand the influence of the initial one million cycles of fatigue loading on the shear performance of RC beams strengthened with FRP sheets, and estimate the fatigue behaviour and crack growth of the RC beams strengthened.

2. Experimental work

Tests were conducted on simply supported short RC beams strengthened with CFRP or GFRP sheets in shear. The beams were tested under static loading and/or fatigue loading to investigate their deflections, strains on the steel rebar, concrete and FRP sheets, crack behaviour as well as shear capacity after one million cycles of fatigue loading.

2.1. Details of test beams, materials and mix

Tests were carried out on five rectangular RC beams reinforced with different patterns and types of FRP sheets. The geometry and reinforcement of the beams tested are shown in Fig. 1. All beams have the same overall cross-sectional dimensions, internal longitudinal reinforcement and stirrup arrangements. The beams are 150 mm wide, 300 mm high and 1700 mm long. The net span of 1500 mm is limited by the testing machine configuration. One of five beams was tested under static load, the rest four were tested under fatigue loading. The ultimate load (P_u) obtained from the static test was used to determine the minimum fatigue loading (P_{min}) and maximum fatigue loading (P_{max}).

Concrete mix was designed with the grade of compressive strength of C30 according to the Chinese Standard [40]. The mix was made of ordinary Portland cement 32.5R, natural sand and gravels with aggregate size between 10 and 31 mm. The water to cement ratio was kept constant at 0.55. Cement, water, fine and coarse aggregates were mixed in their weight proportions of 1:0.55:1.76:3.13. Besides the test beams, six concrete cube specimens with side length of 150 mm were made for compressive strength tests at the time of casting and were kept with the beams during curing. In the sample preparation, all test members were placed on a vibration platform to ensure proper compaction, however special care was taken on the strain gauges attached to steel bars during the vibration. The average of 28-day cube strength was 31.3 MPa.

For all concrete beams, three types of the mild steel bars were used for the longitudinal and the transverse reinforcements. There were two sets of steel smooth bars placed in the tensile and compressive faces of the beam respectively. There were also steel smooth bars placed transversely for the shear reinforcement. The details of the reinforcement and material properties of the rebars (supplied by the Shanxi Zhongyu Ironsteel Co. Ltd.) and concrete are summarized in Fig. 1 and Table 1, respectively.

The FRP materials consist of CFRP and GFRP sheets (supplied by the Shanghai Keep Strong in Building Technology Engineering Co. Ltd.) with a thickness (t_f) of 0.11 and 0.27 mm, respectively. Tensile strength, elastic modulus and ultimate strain of the FRP materials are also given in Table 1.

2.2. The strengthening scheme

All the beams were externally strengthened with a unidirectional CFRP or GFRP sheets, except for the reference beam. Two
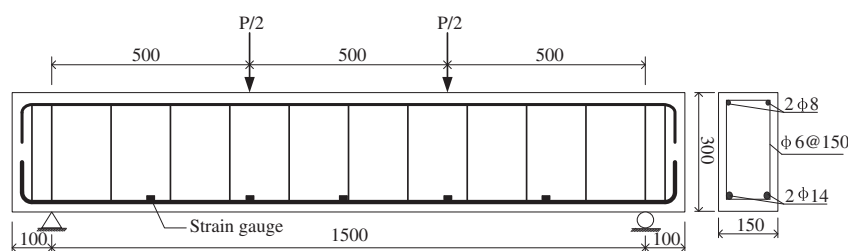

Fig. 1. The geometric, loading and boundary conditions and steel reinforcement of the RC beam.

Table 1
Mechanical properties of the RC beams and FRP materials.

Material	Dimensions (mm)	Yield strength (MPa)	Compressive strength (MPa)	Tensile strength (MPa)	Elastic modulus (GPa)	Ultimate strain (%)
Concrete	C30	–	31.3	–	–	–
Steel	$D = 6$	240	–	420	210	30.0
	$D = 8$	330	–	490	210	28.0
	$D = 14$	410	–	555	200	28.5
CFRP sheets	$t_f = 0.11$	–	–	4103	242	1.7
GFRP sheets	$t_f = 0.27$	–	–	3400	73	2.7
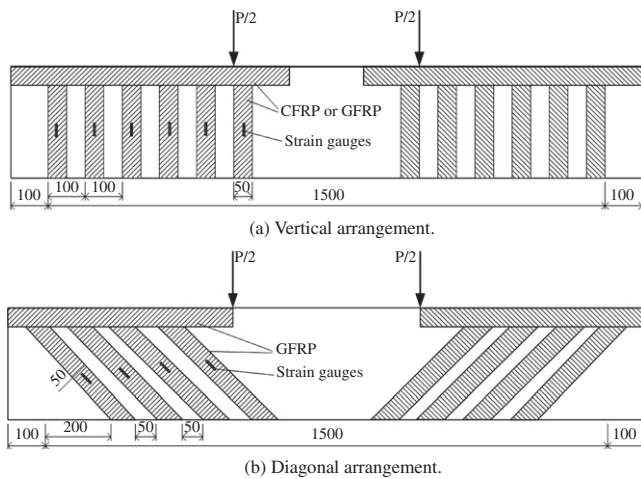
Fig. 2. The reinforcing arrangements of FRP sheets for the beams strengthened.

strengthening orientations were applied in the experimental work, which are shown in Fig. 2. The detailed reinforcing arrangements are listed in Table 2. The beam FCB30 was the reference one subjected to static loading only, and the beam FB30-1 was the beam without attaching any FRP sheet but subjected to fatigue loading for control purpose. The beam FB30-2 was strengthened with one layer CFRP sheets on both the lateral faces and the bottom face of the beam. The beam FB30-3 and the beam FB30-4 were strengthened with one layer GFRP sheets in the form of the vertical bonding and the diagonal bonding, respectively.

Before the strengthening, the concrete surface where FRP sheets to be bonded was being polished until fine aggregates were exposed and then cleaned with pressurized air and acetone. After that, a two-part primer was applied to the prepared concrete surface and left to dry, and then a two-part epoxy resin was applied to the primed concrete surface, followed by bonding of the FRP sheets according to the strengthening arrangements, as shown in Fig. 2.

2.3. Test procedures

The four-point bending was applied to test all beams. The beam surfaces at supports and loading points were smoothened with
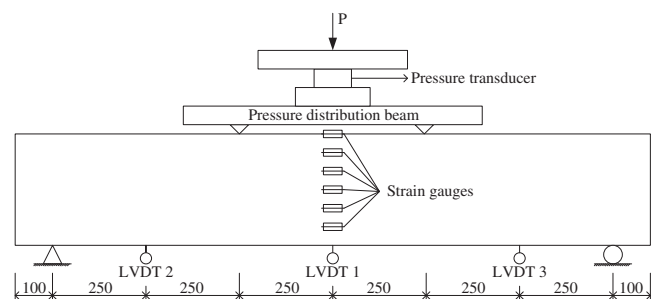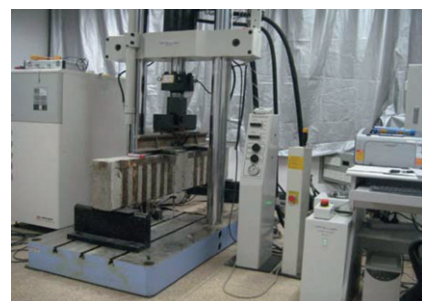
sand-paper to avoid any eccentricity in loading. Also four steel plates (100 mm wide and 20 mm thick) were placed above the supports and underneath the loading points to avoid local crushing on the beams tested. Before casting five strain gauges were attached to the longitudinal steel bars, and prior to the testing five gauges on the concrete surface, and four or six more gauges on the FRP sheets, as shown in Figs. 1–3. Furthermore, three linear voltage displacement transducers (LVDTs) were placed to measure the vertical deflections underneath the mid-span and the mid-shear span of the beams.

The reference beam was tested monotonically to failure to identify the ultimate load (P_u), which was 115.8 kN. All but one of the five beams were first subjected to one million cycles of fatigue loading, and then loaded monotonically up to failure under four-point bending. The minimum and maximum loads, P_{min} and P_{max}, applied were shown in Table 2. A constant load ratio F between P_{min} and P_{max} was used in the test ($F = P_{min}/P_{max} = 0.375$).

The fatigue load was applied through a Shimadzu Fatigue 4890 hydraulic actuator with 200 kN capacity controlled by the Shimadzu Gluon test execution software, as shown in Fig. 3. The maximum load (P_{max}) and the minimum load (P_{min}) during all fatigue cycles were determined at 40% and 15% of the ultimate load of the reference beam, respectively. All fatigue beams were first subjected to two cycles of flexural loading between the zero kN and P_{max} through six increments ($0.2P_{max}$, including P_{min}) up to P_{max} in order to check the testing machine and the data acquisition

Table 2
Details of the FRP reinforcement and fatigue load settings.

Beam	FRP type	FRP layer	FRP angle (°)	Cycles	P_{min} (kN)	P_{max} (kN)	$(P_{min} - P_{max})/P_u$ (%)
FCB30	–	–	–	0	0	0	0
FB30-1	–	–	–	1000,000	17.37	46.32	15–40
FB30-2	CFRP	1	90	1000,000	17.37	46.32	15–40
FB30-3	GFRP	1	90	1000,000	17.37	46.32	15–40
FB30-4	GFRP	1	45/135	1000,000	17.37	46.32	15–40

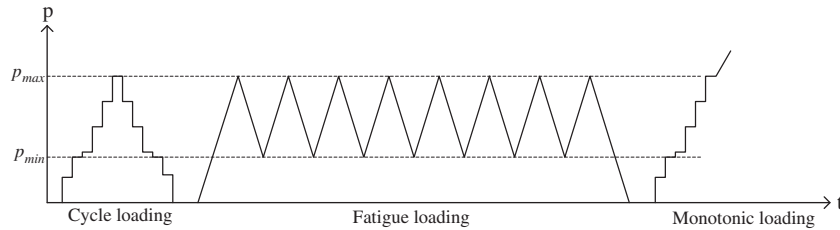**Fig. 3.** The schematic view and the test setup.

Fig. 4. The loading schemes for beams tested.

system. Then all beams were subjected to fatigue loading which was controlled using a form of sinusoidal wave with a frequency of 5 Hz, as shown in Fig. 4.

The tests were terminated at the pre-designed number of fatigue loading cycles, and then the beams were subjected to six cycles of loading and unloading between zero kN and P_{max} at a rate of 0.2 kN/s. This was to measure deflections and strain values on the FRP sheets and on the concrete surface during this loading regime, since deflection and strain data cannot be recorded accurately during a fatigue load cycle [19]. Full cycle readings during the test were taken according to the following intervals: at 0 cycle and every 20th cycle up to 200 cycles; then every 200th cycle up to 2000; every 2000th cycle up to 20,000; every 20,000th cycle up to 200,000; at every 200,000th cycle up to 1000,000. After the fatigue tests, all beams were loaded monotonically up to failure. The monotonic load was applied at the same location as that for the cyclic loading and data were recorded at every 2 kN load increment.

3. Results and discussion

3.1. Failure modes

Fig. 5 shows the ultimate failure modes of all beams tested. The failure mode of the statically loaded reference beam FCB30 was a typical shear failure, i.e. the failure occurred suddenly by formation of a diagonal crack near the support propagating to a loading point, as shown in Fig. 5a. For the non-strengthened beam FB30-1, which was subjected to one million fatigue cycles, there was a major diagonal crack developed first along the longitudinal axis from the mid-shear span towards the top of the beam and then extended approaching to a loading point. As a result, the major flexural cracks were developed for the beam FB30-1 at the ultimate load (Fig. 5b), which was due to the influence of fatigue loading on tensile strength of the longitudinal bars. For beams FB30-2 to FB30-4, which were strengthened by FRP sheets and subjected to one million fatigue cycles, the failure modes obtained from the subsequent monotonic failure tests were changed from a brittle shear failure to a ductile flexural failure, as shown in Fig. 5c–e. Beams FB30-2 and FB30-3 which were strengthened with perpendicular CFRP or GFRP sheets demonstrated some control on crack growth and introduced more cracks up to the failure. This was due to the favorable properties of CFRP and GFRP in fatigue [24]. However, a diagonal crack was developed firstly in the beam FB30-3, followed by the major flexural crack developed from the pure bending section and extended to the top of the beam until the major diagonal crack was developed near the support which caused the ultimate failure. For the beam FB30-4 strengthened with diagonal GFRP sheets, it showed more flexural behaviour than FB30-2 and FB30-3. Therefore, it is noted that the flexural failure is prominent when the beams are strengthened with FRP sheets, and the diagonal bonding of GFRP sheets on the lateral faces of a beam is an effective way to enhance the shear capacity and restrict crack growth.

3.2. First crack load and deflection

The loads corresponding to the first crack for the reference beam and the FRP strengthened beams under monotonic and fatigue loading, together with the ultimate loads, are shown in Table 3. The first crack loads for FB30-2 and FB30-3 were slightly higher than that of the non-strengthened beam FB30-1. The beam FB30-2 that was strengthened by CFRP showed a higher first crack load than that of the GFRP strengthened beam FB30-3 due to the superior property of CFRP in strength. However, the beam strengthened with diagonal GFRP sheets gave the highest first crack load of 45.95 kN, which was 24.7% higher than that of the non-strengthened beam FB30-1.

When the beams subjected to the fatigue loading, the loads on which the number of new cracks were developed (Table 3) were increased significantly. Such the loads for beams strengthened with GFRP sheets, i.e. FB30-3 and FB30-4, were 2.5% and 11.3% higher than that of the non-strengthened beam FB30-1, respectively. However the beam strengthened with CFRP sheets (FB30-2) gave the highest new crack load, due to the better mechanical properties of CFRP in comparison to GFRP. However, the ultimate strengths of FB30-1 and FB30-3 were 5.5% and 2.2% lower than that of the reference beam, which was likely caused by the accumulated fatigue damage before the final monotonous loading (FB30-1) and the partial debonding of GFRP sheets during the final monotonous test (FB30-3). Furthermore, such the strengths for FB30-2 and FB30-4 were 4.5% and 2.6% higher than that of the reference beam FCB30. In addition, the FRP strengthened beams, FB30-2, FB30-3 and FB30-4, showed a lower ultimate deflection than that of the non-strengthened beam FB30-1 by 70%, 33% and 18%, respectively. The results in Table 3 indicate that the CFRP strengthened beam (FB30-2) give the highest ultimate load but the lowest deflection whereas the beam strengthened with diagonal GFRP reinforcing arrangement (FB30-4) is more effective than the vertical GFRP one (FB30-3) in terms of the ultimate load and ductility.

Load–deflection curves for all beams presented in Table 3 are shown in Fig. 6. As can be seen, load and deflection are increased almost proportionally up to the first crack load. There are clear differences between the initial stiffness for the FRP strengthened beams and the non-strengthened beam and the reference beam. As FRP strengthened beams, FB30-2, FB30-3 and FB30-4 show the higher stiffness over the virgin beam FCB30 and the non-strengthened beam FB30-1, however, the stiffness for FB30-2 and FB30-4 is pretty similar. Regarding the bending stiffness, the above results have again revealed that 45° bonding arrangement (FB30-4) is more effective than the vertical bonding one. As it can be observed for the beams subjected to fatigue loading, there is no obviously peak load. It is likely that due to fatigue loading some small cracks already occurred in those beams before the ultimate failure tests were carried out [26]. The improvement on performance of the beam FB30-4 was attributed to the effectiveness of the diagonally bonded GFRP sheets which control the growth of small cracks and reduce strains on the concrete. The similar phenomena were

(a) FCB30.

(b) FB30-1.

(c) FB30-2.

(d) FB30-3.

(e) FB30-4.

Fig. 5. Failure modes of the beams tested.

Table 3
Test results of all beams tested.

Beam	Initial crack load in fatigue (kN)	New crack load in post-fatigue (kN)	Ultimate load (kN)	Deflection (mm)	Failure mode
FCB30	–	35.05	115.81	8.55	A
FB30-1	36.85	76.35	109.39	11.40	B
FB30-2	37.02	89.01	121.06	3.41	C
FB30-3	36.89	78.26	113.94	7.61	D
FB30-4	45.95	84.95	118.88	9.32	C

A is shear failure; B is flexural failure and concrete good; C is flexural failure and concrete crushing; D is shear failure and concrete good.

also observed by Leung et al. [29], who studied the layered ECC concrete beams subjected to static and fatigue loads.

3.3. Test results under the fatigue loading

Adopting the similar presentation approach by Teng et al. [17], the following charts are produced to describe the fatigue behaviour obtained, i.e. load–deflection, deflection-fatigue cycle number, and strains on the concrete, FRP and steel versus fatigue cycle number respectively. The deflection and strain readings were taken during cyclic monotonic tests after the fatigue loading, as indicated in Fig. 4.

The mid-span deflections and strains recorded are shown in Figs. 7 and 8 and Table 4. Fig. 7 shows relationships between the load and the mid-span deflection for all fatigue beams. Seven curves are plotted to represent the load–deflection behaviour of the beam at different cyclic intervals from the beginning to the final cycle of the fatigue loading. The mid-span deflections of FB30-1
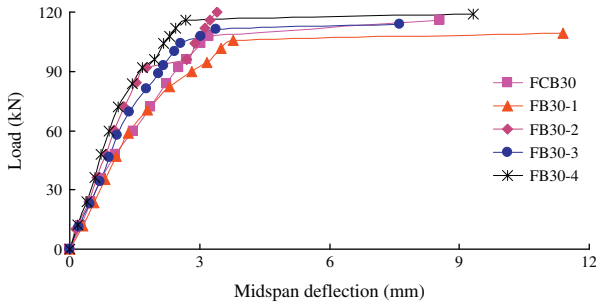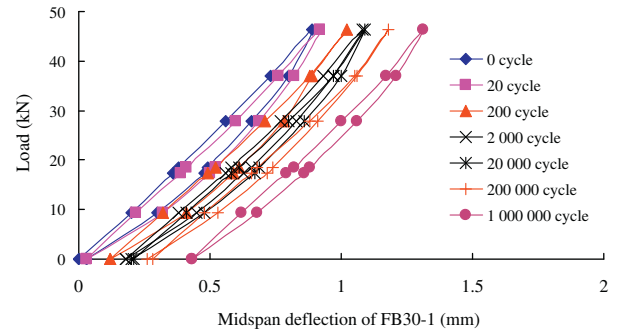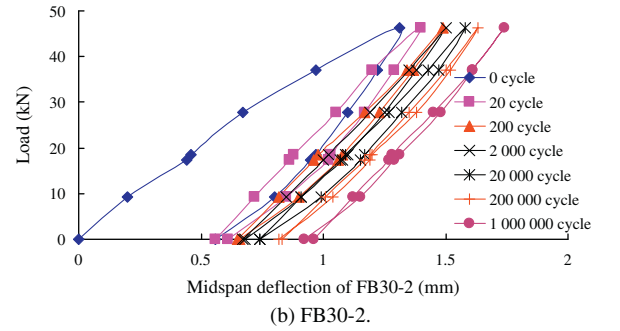
Fig. 6. Load–deflection curves of beams tested.

and FB30-2 (Fig. 7a and b) gradually increase with the number of fatigue cycles, however, there is no such a trend for FB30-3 and FB30-4 (Fig. 7c and d) after the initial a few hundred cycles of the fatigue loading. The initial deflections of FB30-2, FB30-3 and FB30-4 at the first twenty cycles are 0.56, 0.39 and 0.33 mm, respectively, which might be caused by the slipping/engaging of FRP sheet during the initial fatigue loading (Fig. 7b–d). The deflection difference between the zero cycle and one millionth cycle for the beam FB30-1 at the zero load is 0.43 mm, which is 16%, 63% and 86% higher than the corresponding differences for FB30-2 (0.36 mm), FB30-3 (0.16 mm) and FB30-4 (0.06 mm), respectively. Table 4 gives the deflections at the beginning and the end of the fatigue tests. Compared to the preloading phase, deflections of FB30-1, FB30-2, FB30-3 and FB30-4 when subjected to one million fatigue cycles are reduced by 2%, 46%, 43% and 55%, respectively. Once again, the main reason for beam strengthened with 45° GFRP sheets to have the most reduction on the deflection after one million fatigue cycles might be that the stiffness of the beam FB30-4 was improved greatly by the diagonal reinforcing arrangement that increases the effective strains on the GFRP sheets, as shown in Fig. 8b. Therefore, this indicates that the beam strengthened by the diagonal bonding of GFRP sheets (FB30-4) has the highest stiffness and the diagonal strengthening arrangement of GFRP sheets is the most effective way to enhance the strength of beam when subjected to fatigue loading.

Strains on the concrete, FRP and steel were recorded to investigate how different strengthening materials (GFRP or CFRP) and methods (vertical or diagonal bonding arrangements) influence this parameter under the fatigue loading. For the non-strengthened beam FB30-1, strains on the concrete were increased greatly up to the 200,000th cycle, then gradually increased up to the 800,000th cycle and increased significantly again to the end of the test (Fig. 8a). But such the strains on the steel were increased steadily with the fatigue cycle number between the zero cycle and the 600,000th cycle and then were risen mildly to the one millionth cycle (Fig. 8c). However, the strains on the concrete and steel for the FRP strengthened beams, FB30-2, FB30-3 and FB30-4, showed a different trend. As it can be seen in Fig. 8a, strains on the concrete for FB30-2 and FB30-4 were increased steadily with increasing fatigue cyclic number throughout the fatigue tests. However, such the strains for the beam FB30-3 were initially increased up to the 200,000th cycle, then gradually decreased up to the 800,000th cycle and increased again to the end of the test. This might be caused by possible slipping and engaging between the vertically bonded GFRP sheets and concrete. The strains on the steel for the vertically bonded FRP beams (FB30-2 and FB30-3) were changed a little after the initial increasing during the first 400,000 cycles (Fig. 8c). However, such the strains for the diagonally bonded GFRP beam (FB30-4) were only mildly increased for the first 800,000 cycles, and then decreased mildly. This was likely due to the strong diagonal reinforcement in the first stage and subsequent partially losing load
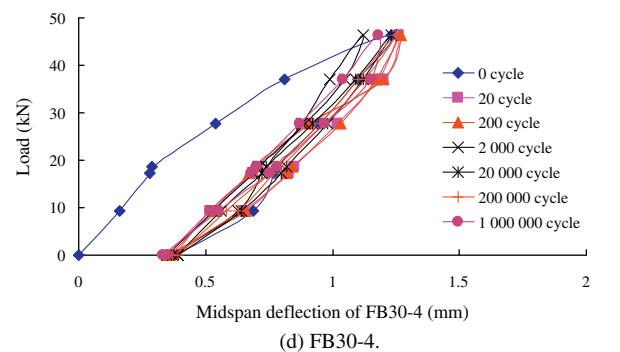

(a) FB30-1.

(b) FB30-2.
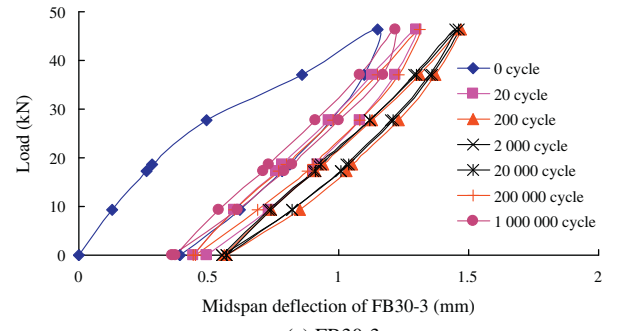
(c) FB30-3.

(d) FB30-4.

Fig. 7. Load–deflection curves of beams tested under fatigue.

carrying capacity of the reinforcement caused by gradual debonding. As can be seen in Fig. 8b, the strains on the diagonally bonded GFRP sheets for the beam FB30-4 were fluctuated throughout the test, which was likely caused by such reinforcing pattern, i.e. some relaxation and re-engaging occurring. Such the strains related to the beam FB30-2 were increased in the first 400,000 cycles and then hardly changed afterwards, whilst such the strains for the beam FB30-3 were increased up to the 200,000th cycle and then into a mild down-up stage.
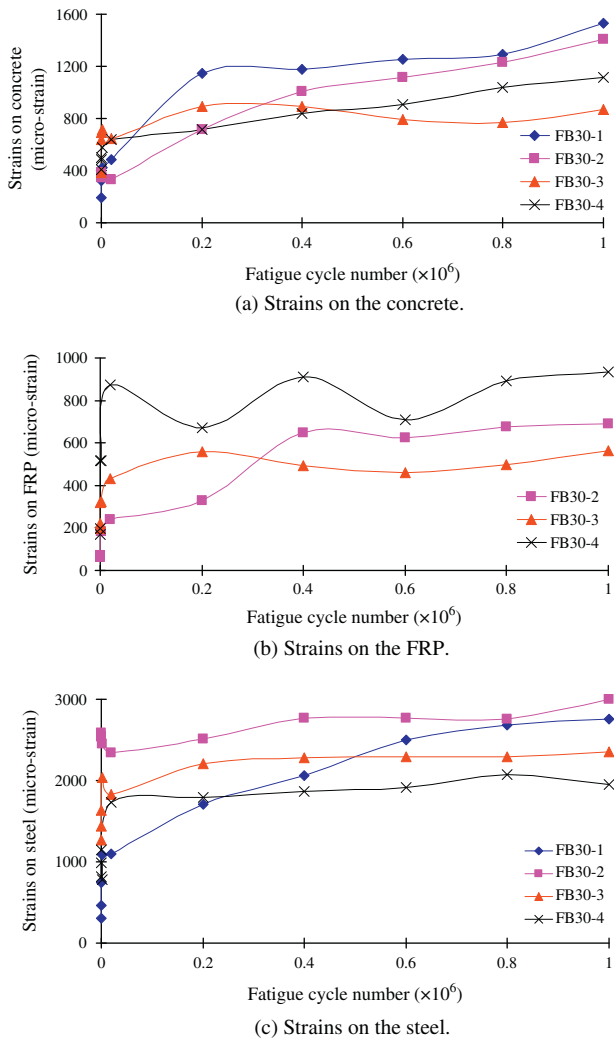
(a) Strains on the concrete.

(b) Strains on the FRP.

(c) Strains on the steel.

Fig. 8. Strains recorded on the concrete, FRP and steel of beams tested at peak load.

Table 4
Comparisons of the mid-span deflection readings at the beginning and the end of the fatigue tests.

Deflection at midspan (mm)	At the beginning of fatigue cycles			After 1 million fatigue cycles		
	17.37 kN (P_{min})	46.32 kN (P_{max})	Δ	17.37 kN (P_{min})	46.32 kN (P_{max})	Δ
FB30-1	0.36	0.89	0.53	0.79	1.31	0.52
FB30-2	0.44	1.31	0.87	1.27	1.74	0.47
FB30-3	0.26	1.15	0.89	0.71	1.22	0.51
FB30-4	0.28	1.23	0.95	0.41	0.84	0.43

3.4. Test results of the ultimate monotonic loading after fatigue cycles

Following the fatigue cyclic load, all beams were loaded monotonically to failure. Fig. 9 shows the load–strain relationships measured on the concrete (compression zone), FRP and steel during the post-fatigue monotonous loading for all beams tested. As shown in Fig. 9a, the initial stiffness related to strains on the concrete for all beams tested, except for the beam FB30-2, were similar before 45 kN. After the load exceeded 45 kN, the maximum compressive strains on the concrete for FB30-2 and FB30-4 were smaller than those on the non-strengthened beam FB30-1 and the reference beam FCB30 for a given load until failure. Also the beam

strengthened with diagonal GFRP sheets (FB30-4) had the lowest compressive strains which was likely caused by the superior sheet thickness and the strong diagonal arrangement of GFRP in shear and fatigue performance in comparison to CFRP [1,12]. However, such the strains for the beam FB30-3, strengthened with vertical GFRP sheets, had similar values to the non-strengthened beam FB30-1 up to the load of 70 kN and then were reduced slightly until the failure. In addition, the measured strains on the concrete for the beam FB30-1 were smaller than that of the beam FCB30 for a given load between 55 kN and 102 kN, but then in a mild increasing trend. This might be caused by the accumulative damage on beam FB30-1 during the one million fatigue cycles. As shown in Fig. 9b, the strains recorded on the FRP sheets were in the descending order corresponding to FB30-2, FB30-3 and FB30-4, which is understandably related to the strengthening materials and reinforcing arrangements. Initially the lowest strain was recorded on the CFRP sheets for the beam FB30-2 up to 40 kN, since CFRP is stiffer than GFRP. However, for a load up to 90 kN the strains on the diagonally bonded GFRP sheets (FB30-4) were greater than those
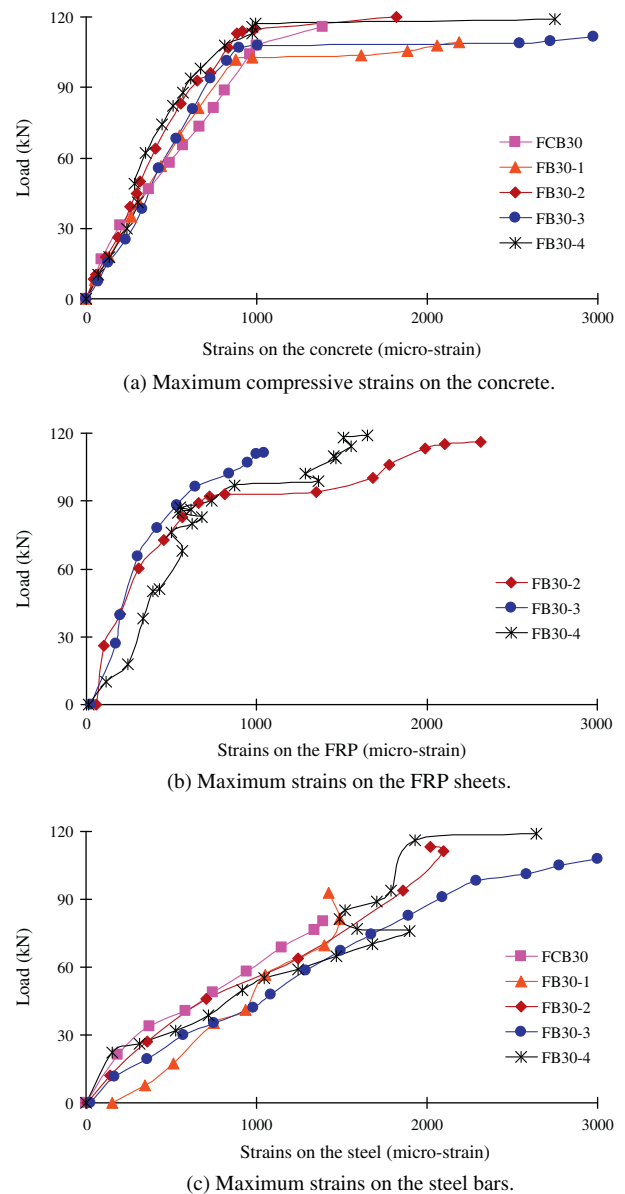

(a) Maximum compressive strains on the concrete.

(b) Maximum strains on the FRP sheets.

(c) Maximum strains on the steel bars.

Fig. 9. Load–strain curves of beams tested under the post-fatigue monotonous load.

on the vertically bonded CFRP and GFRP sheets (FB30-2 and FB30-3) as the former reinforcing pattern provided a better bonding strength than the latter due to a larger bonding area. As a result, higher strains were recorded on the diagonal GFRP sheets which were well bonded to the concrete and shared a higher loading than the vertically bonded FRP sheets until debonding occurred eventually. The evolution of strains on the steel bar showed that such the strains on all beams strengthened were increased more than those on the non-strengthened beams. Moreover, the strains on the steel for the beam FB30-3 were increased more than those for FB30-2 and FB30-4, since the beam strengthened by vertical GFRP sheets was less stiff than the similarly strengthened beam by CFRP and the beam strengthened by the diagonally bonded GFRP sheets.
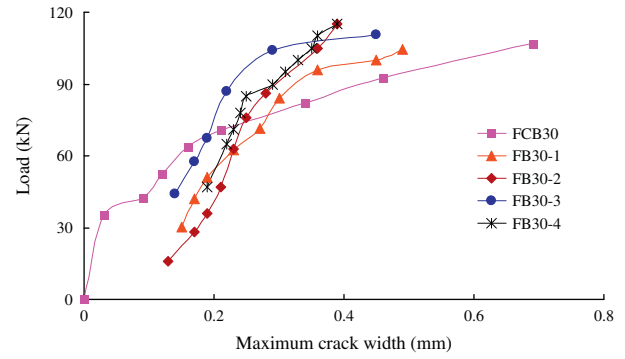
For the concrete beams tested within this study, crack widths were measured after every loading increment by the PTS-C10 crack width measuring device. The detailed measurements on cracks and the relationship between the load and the corresponding maximum crack width measured through monotonous load tests are shown in Table 5 and Fig. 10, respectively. The crack widths shown in Table 5 were measured after the beams failure, i.e. the ultimate values, whilst those shown in Fig. 10 were obtained through manual measurements during the test. Once the crack growth rate becomes accelerated the subsequent measurements cannot be done manually. It can be seen that the FRP strengthened beams have a smaller crack width than that of the reference beam (FCB30), and exhibit a fewer number of cracks in comparison to the beam FB30-1 (Table 5). These results were similar to those obtained from the experimental tests under static four-point bending loading [1,3,12,13]. For the reference beam FCB30, the initial crack width was increased mildly from zero load to 35 kN, then risen more to 42 kN, followed by a steady increase until failure. This was caused by the yield of steel bars. The maximum crack widths measured under monotonous loading for the beams, FB30-1, FB30-2, FB30-3 and FB30-4 were larger than that of the reference beam (FCB30) before the load of 67 kN, due to accumulation of damage throughout the one million fatigue cycles. After the load exceeded the yield of steel, the crack growth on the FRP strengthened beams was slowed down, which was overtaken by the non-strengthened beam FB30-1 and the reference beam FCB30. This was likely contributed by the FRP sheets that limited the crack growth on the FRP strengthened beams, which was also reflected by the rapid increasing of the strains on the FRP sheets (Fig. 9b). However, up to the load of 104 kN the maximum crack width on the beam FB30-3, which was strengthened by the vertical GFRP sheets, had a smaller crack width than that of the beam FB30-4 strengthened with the diagonal GFRP sheets. This was related to the major crack in FB30-3 close to the support but to the crack in FB30-4 close to the midspan, as shown in Table 5. Beyond 104 kN, the crack in the beam FB30-3 was developed more quickly than that on the beam FB30-4, as shown in Fig. 10.

4. Estimate shear capacities of the reinforced beams tested

Generally, analysis of the shear capacity of the beams tested is more complicated than that of the flexural behaviour. The theoretical

Fig. 10. Measured crack width of beams tested during the post-fatigue monotonous loading.

approach for analyzing the shear behaviour is based on developing empirical formulas from the experimental results and simplified assumptions. There are numbers of parameters that affect the shear capacity, such as loading history, presence of cracks, non-linearity and non-homogeneity of the concrete, etc. In general, the shear capacity of a beam strengthened with FRP materials, V^{ana}, can be computed by summarising the shear strength contributions from the concrete, steel reinforcement and FRP. Therefore, the nominal shear strength of the RC beam reinforced by FRP can be expressed as follows [27,28,33]

$$V^{ana} = V_c + V_s + V_f \qquad (1)$$

where V_c, V_s, and V_f represent the shear strength provided by the concrete, stirrups and FRP sheet, respectively.

In research of the behaviour and performance of RC beams externally strengthened in shear with CFRP, Lee et al. [41] investigated the concrete contribution in shear strength through the comparative study of the ACI design model [42] and the CIRIA design model [43]. They have indicated that the calculations for the concrete contribution based on the CIRIA the model correlates well to the experimental results, which is shown as

$$V_c = 0.44 \cdot (1 - 0.35 \cdot a/d) \cdot \sqrt{f_{cu}} \cdot b \cdot d \qquad (2)$$

where a is the effective clear shear span, d is the effective depth of the cross section, f_{cu} is the cube compressive strength of concrete, b is the beam width.

The stirrups contribution was studied by Kim et al. [18], Rangan [44] and Cladera and Marí [45], which is given in SI units as

$$V_s = \frac{A_v \cdot f_y \cdot d}{s \cdot \tan \theta} \qquad (3)$$

where A_v is the cross sectional area of the shear reinforcement, s is the spacing of the stirrups, f_y is the design yield strength of the shear reinforcement and θ is the critical shear crack angle with respect to the beam longitudinal axis.

For the reference beam FCB30 and the non-strengthened beam FB30-1, the shear carrying capacities obtained by Eqs. (2) and (3), and the ratios of those estimated values to the experimental ones are shown in Table 6. It can be seen that the shear capacities of the reference beam obtained by experiment and by the theoretical estimation are correlated reasonably well, i.e. the ratio is close to 1. However, for the non-strengthened beam FB30-1, which was subjected to one million fatigue cycles, its experimental value is lower than that of the estimated one since the accumulated fatigue damage was not considered here. In order to take the fatigue damage into account, damage factors λ_s and λ_f are introduced to take the fatigue effects on the steel and the FRP into account. Although such factors consider the individual damage accumulations from the

Table 5
Data of cracks at failure for all beams tested.

Beam	Maximum width (mm)	Crack end from the bottom (mm)	Distance from support (mm)	Numbers
FCB30	8.3	216	600	8
FB30-1	6.0	264	615	9
FB30-2	4.5	247	560	7
FB30-3	7.5	240	295	6
FB30-4	8.0	286	740	6

steel and the FRP, the highly-weighted contribution is from the FRP as there are possible delamination, fibre break and de-bonding caused by fatigue. Therefore, the shear capacities of FRP strengthened beams subjected to one million fatigue cycles may be estimated as

$$V^{ana} = V_c + \lambda_s \cdot V_s + \lambda_f \cdot V_f \tag{4}$$

The shear strength contribution provided by the FRP sheets is calculated according to the studies carried out by Lee et al. [41], which is based on the studies of the ACI [46] and the combined influence of the elastic modulus, the reinforcement ratio of FRP and inclination of FRP sheets.

$$V_f^I = \rho_f \cdot (\sin \beta + \cos \beta) \cdot E_f \cdot R \cdot \varepsilon_{fu} \cdot b \cdot d_f \tag{5}$$

To investigate shear carrying capacities of the textile reinforced concrete beams, Larbi et al. [47] also proposed the FRP shear contribution as

$$V_f^{II} = 0.9 \cdot \rho_f \cdot (\cot \theta + \cot \beta) \cdot \sin \beta \cdot E_f \cdot R \cdot \varepsilon_{fu} \cdot b \cdot d_f \tag{6}$$

In addition Perera et al. [48] proposed the following equation to count in the FRP contribution and to represent more suitable dependence on the reinforcement ratio of the beams strengthened.

$$V_f^{III} = c_1 \cdot \rho_f^{c_2} \cdot (\sin \beta + \cos \beta) \cdot E_f \cdot R \cdot \varepsilon_{fu} \cdot b \cdot d_f \tag{7}$$

where c_1 and c_2 are unknown parameters to be determined by solving a minimization problem of the objective function defined from the difference between the experimental results and the estimated values by Eqs. (5) and (6). The final form is shown as

$$V_f^{III} = 1.97 \cdot \rho_f^{1.11} \cdot (\sin \beta + \cos \beta) \cdot E_f \cdot R \cdot \varepsilon_{fu} \cdot b \cdot d_f \tag{8}$$

According to the theoretical prediction of FCB30 and the experimental result of FB30-1, the value of λ_s can be set as 0.89, which is the ratio of experimental reduction of FB30-1 due to the one million fatigue cycles to the theoretical prediction of FCB30. Based on the previous research work [15,24,28,31,36], the fatigue damage factor of the FRP sheet (λ_f) is related to the fatigue load ratio (F), the applied fatigue frequency (H), the FRP reinforcing arrangement angle (β) and the elongation of FRP applied (η_f). In addition, Gheorghiu et al. [21,26] have indicated that there is no clear influence of the fatigue cycles on the post-fatigue monotonic strength. Therefore, in this study the fatigue damage factor is proposed as

$$\lambda_f = \frac{1}{F} \cdot \frac{1}{H} \cdot \cos \frac{\beta}{2} \cdot \frac{1}{\eta_f} \tag{9}$$

In the above equations, ρ_f is the FRP area fraction and equal to $2(t_f/b)(w_f/s_f)$, d_f is the effective depth of FRP sheets, t_f is the thickness of FRP sheets, w_f is the width of FRP sheets, s_f is the spacing of FRP sheets, E_f is the elastic modulus of FRP sheets, ε_{fu} is the ultimate strain of FRP sheets. R is the reduction factor in relation to the FRP failure mode, which can be determined as

$$R = 0.39 \cdot (\rho_f \cdot E_f)^2 - 0.85 \cdot \rho_f \cdot E_f + 0.55 \tag{10}$$

The maximum value of R recommended by Sundarraja and Rajamohan [1] is $0.006/\varepsilon_{fu}$ for the FRP-strengthened beams failed by fracturing of the FRP sheets. However, Jayaprakash et al. [49] and El-Ghandour [50] indicated the maximum value of $0.004/\varepsilon_{fu}$ should be appropriate to estimate the shear capacity of beams strengthened. Larbi et al. [47] suggested that the maximum value of R should be equal to 0.5 in Eq. (6). For the FRP strengthened beams in this study, the values obtained by Eqs. (5)–(8), and the ratio of V^{exp}/V^{ana} are also shown in Table 6. Here the value of θ is taken as the default value of 45°. It can be seen that the analytical predictions to evaluate the shear capacities of beams strengthened with FRP sheets is intricate. Although the predictions shown in Table 6 are quite promising, extensive experimental and numerical work need to be carried out to develop comprehensive analytical formulation.

The results show that the external FRP reinforcement improves the fatigue bahaviour of the RC beams, however the fatigue loading induces the reduction of the ultimate load carrying capacity of the RC beams. Although the slippage between the FRP and the concrete reduces the strain on the FRP at the early fatigue stage, the behaviour of the FRP – concrete interface does not challenge the overall post-fatigue behaviour of the FRP retrofitted RC beams.

5. Conclusions

Experimental work has been undertaken to study the fatigue related structural behaviour of RC beams strengthened with FRP sheets. The outcomes of the experimental work on RC beams strengthened with FRP sheets (CFRP and GFRP) have proved the efficiency of strengthening arrangements when subjected to fatigue loading. The test results have shown that externally bonded CFRP or GFRP to the lateral and bottom faces of a beam can increase the first crack load and ultimate strength greatly, arrest concrete crack extension, and enhance the rigidity of strengthened beams. The FRP strengthened beams have exhibited more widely spaced and a fewer number of cracks in comparison to the reference beam. The CFRP strengthened beam has the highest ultimate strength but the lowest deflection, and the diagonal GFRP reinforcing arrangement is more effective than the vertical arrangement in enhancing the shear strength and stiffness. Moreover, the FRP strengthened beams show the lower ultimate deflection than the non-strengthened beam by 18–70% when subjected to 1000,000 cycles of fatigue loading. Post-fatigue monotonic tests have showed that load–deflection responses of the beams with and without previous fatigue loading are very similar until the final failure stage. However, the stiffness of CFRP-strengthened beam is degraded more greatly than GFRP-strengthened beam after one million fatigue cycles. The beam which reinforced by bonding diagonal GFRP sheets has the highest first crack load, which is 24.7% higher than that of the reference beam. In addition shear capacities of the beams tested are estimated quite well.

Acknowledgements

References

[1] Sundarraja MC, Rajamohan S. Strengthening of RC beams in shear using GFRP inclined strips – an experimental study. Constr Build Mater 2009;23:856–64.
[2] Wang YC, Hsu K. Design recommendations for the strengthening of reinforced concrete beams with externally bonded composite plates. Compos Struct 2009;88:323–32.

Table 6
Comparisons between the experimental results and the theoretical predictions of the shear capacities at failure.

Beam	V^{exp} (kN)	Lee et al. [36]		Larbi et al. [42]		Perera et al. [43]	
		V^{ana} (kN)	V^{exp}/V^{ana}	V^{ana} (kN)	V^{exp}/V^{ana}	V^{ana} (kN)	V^{exp}/V^{ana}
FCB30	57.91	57.21	1.01	57.21	1.01	57.21	1.01
FB30-1	54.70	54.57	1.00	54.57	1.00	54.57	1.00
FB30-2	60.53	60.89	0.99	60.26	1.00	60.20	1.01
FB30-3	56.97	57.52	0.99	57.23	1.00	57.48	0.99
FB30-4	59.44	60.02	0.99	59.48	1.00	59.94	0.99

[3] Dong JF, Wang QY, Qiu CC, Zhu YM, Yan HQ. Experimental study on fracture properties of concrete beams strengthened with externally bonded CFRP sheets. China Civ Eng J 2010;43(S2):76–82. in Chinese.

[4] Wang W, Wu SG, Dai HZ. Fatigue behavior and life prediction of carbon fiber reinforced concrete under cyclic flexural loading. Mat Sci Eng A 2006;434:347–51.

[5] Dong JF, Wang QY, Zhu YM, Qiu CC. Experimental study on RC beams strengthened with externally bonded FRP sheets. J Sichuan Uni (Eng Sci) 2010;42(5):197–203. in Chinese.

[6] Maaddawy TE, Sherif S. FRP composites for shear strengthening of reinforced concrete deep beams with opening. Compos Struct 2009;89:60–9.

[7] Zhao XL, Al-mahaidi R. Wenchuan post-earthquake reconstruction by utilizing composite tubular construction and FRP retrofitting technology. J Sichuan Uni (Eng Sci) 2009;41(3):231–47.

[8] Wang W, Dai HZ, Wu SG. Mechanical behavior and electrical property of CFRC-strengthened RC beams under fatigue and monotonic loading. Mat Sci Eng A 2008;479:191–6.

[9] Deng J, Lee MMK. Fatigue performance of metallic beam strengthened with a bonded CFRP plate. Compos Struct 2007;78:222–31.

[10] Ferrier E, Bigaud D, Clement JC, et al. Fatigue-loading effect on RC beams strengthened with externally bonded FRP. Constr Build Mater 2011;25:539–46.

[11] Wang QY, Pidaparti RM. Static characteristics and fatigue behavior of composite-repaired aluminium plates. Compos Struct 2002;56:151–5.

[12] Barris C, Torres L, Turon A, et al. An experimental study of the flexural behaviour of GFRP RC beams and comparison with prediction models. Compos Struct 2009;91:286–95.

[13] Maalej M, Leong KS. Effect of beam size and FRP thickness on interfacial shear stress concentration and failure mode of FRP-strengthened beams. Compos Sci Technol 2005;65:1148–58.

[14] Barros JAO, Dias SJE, Lima JLT. Efficacy of CFRP-based techniques for the flexural and shear strengthening of concrete beams. Cement Concrete Compos 2007;29:203–17.

[15] Rteil AA, Soudki KA, Topper TH. Preliminary experimental investigation of the fatigue bond behavior of CFRP confined beams. Constr Build Mater 2007;21:746–55.

[16] Noll T, Magin M, Himmel N. Fatigue life simulation of multi-axial CFRP laminates considering material non-linearity. Int J Fatigue 2010;32:146–57.

[17] Teng JG, Yuan H, Chen JF. FRP-to-concrete interfaces between two adjacent cracks: theoretical model for debonding failure. Int J Solids Struct 2006;43:5750–78.

[18] Kim G, Sim J, Oh H. Shear strength of strengthened RC beams with FRPs in shear. Constr Build Mater 2008;22:1261–70.

[19] Marfia S, Rinaldi Z, Sacco E. Softening behavior of reinforced concrete beams under cyclic loading. Int J Solids Struct 2004;41:3293–316.

[20] Wang YC, Lee MG, Chen BC. Experimental study of FRP-strengthened RC bridge girders subjected to fatigue loading. Compos Struct 2007;81:491–8.

[21] Gheorghiu C, Labossiere P, Proulx J. Fatigue and monotonic strength of RC beams strengthened with CFRPs. Compos Part A – Appl S 2006;37:1111–8.

[22] Liu HB, Xiao ZG, Zhao XL, et al. Prediction of fatigue life for CFRP-strengthened steel plates. Thin Wall Struct 2009;47(10):1069–77.

[23] Tsouvalis NG, Mirisiotis LS, Dimou DN. Experimental and numerical study of the fatigue behaviour of composite patch reinforced cracked steel plates. Int J Fatigue 2009;31:1613–27.

[24] Czaderski C, Motavalli M. Fatigue behavior of CFRP L-shaped plates for shear strengthening of RC T-beams. Compos Part B – Eng 2004;35:279–90.

[25] Ceroni. Experimental performances of RC beams strengthened with FRP materials. Constr Build Mater 2010;24:1547–59.

[26] Gheorghiu C, Labossiere P, Proulx J. Response of CFRP-strengthened beams under fatigue with different load amplitudes. Constr Build Mater 2007;21:756–63.

[27] Nanni A. Fatigue behavior of steel fiber reinforced concrete. Cement Concrete Compos 1991;13:239–45.

[28] Chang D, Chai WK. Flexural fracture and fatigue behavior of steel-fiber-reinforced concrete structures. Nucl Eng Des 1995;156:201–7.

[29] Leung CKY, Cheung YN, Zhang J. Fatigue enhancement of concrete beam with ECC layer. Cement Concrete Res 2007;37:743–50.

[30] Manfredi G, Pecce M. Low cycle fatigue of RC beams in NSC and HSC. Eng Struct 1997;19(3):217–23.

[31] Deng ZC. The fracture and fatigue performance in flexure of carbon fiber reinforced concrete. Cement Concrete Compos 2005;27:131–40.

[32] Singh SP, Kaushik SK. Fatigue strength of steel fibre reinforced concrete in flexure. Cement Concrete Compos 2003;25:779–86.

[33] Zhang J, Stang H, Li VC. Fatigue life prediction of fiber reinforced concrete under flexural load. Int J Fatigue 1999;21:1033–49.

[34] Cheng L. Flexural fatigue analysis of a CFRP form reinforced concrete bridge deck. Compos Struct 2011;93:2895–902.

[35] Chen D, El-Hacha R. Behaviour of hybrid FRP-UHPC beams in flexure under fatigue loading. Compos Struct 2011;94:253–66.

[36] Kwak KH, Kim JJ. Fatigue strength in polymer-reinforced concrete beams under cyclic loading. Nucl Eng Des 1995;156:63–73.

[37] Lu F, Ayoub A. Evaluation of debonding failure of reinforced concrete girders strengthened in flexure with FRP laminates using finite element modeling. Constr Build Mater 2011;25:1963–79.

[38] Yun Y, Wu YF, Tang WC. Performance of FRP bonding systems under fatigue loading. Eng Struct 2008;30:3129–40.

[39] Carloni C, Subramaniam KV, Savoia M, Mazzotti C. Experimental determination of FRP-concrete cohesive interface properties under fatigue loading. Compos Struct 2011. http://dx.doi.org/10.1016/j.compstruct.2011.10.026.

[40] Ministry of Construction. Code for design of concrete structures, GB: 50010, Ministry of Construction, PR China; 2002.

[41] Lee HK, Cheong SH, Ha SK, et al. Behavior and performance of RC T-section deep beams externally strengthened in shear with CFRP sheets. Compos Struct 2011;93:911–22.

[42] ACI Committee 318. Building code requirements for reinforced concrete and commentary [ACI 318–95, ACI 318R–95]. American Concrete Institute, Farmington hills; 1998.

[43] Construction Industry Research and Information Association. CIRIA GUIDE 2: the design of deep beams in reinforced concrete. Ove Arup and Partners and CIRIA, London; 1997.

[44] Rangan BV. Shear design of reinforced concrete beams, slabs and walls. Cement Concrete Compos 1998;20:455–64.

[45] Cladera A, Marí AR. Shear design procedure for reinforced normal and high-strength concrete beams using artificial neural networks. Part II: beams with stirrups. Eng Struct 2004;26:927–36.

[46] ACI 440.2R-02. Guild for the design and construction of externally bonded FRP systems for strengthening concrete structures. Reported by ACI Committee 440. American Concrete Institute, Farmington Hills, Michigan (USA); 2002.

[47] Larbi AS, Contamine R, Ferrier E, Hamelin P. Shear strengthening of RC beams with textile reinforced concrete (TRC) plate. Constr Build Mater 2010;24:1928–36.

[48] Perera R, Arteaga A, Diego AD. Artificial intelligence techniques for prediction of the capacity of RC beams strengthened in shear with external FRP reinforcement. Compos Struct 2010;92:1169–75.

[49] Jayaprakash J, Samad AAA, Abbasovich AA, Ali AAA. Shear capacity of precracked and non-precracked reinforced concrete shear beams with externally bonded bi-directional CFRP strips. Constr Build Mater 2008;22:1148–65.

[50] El-Ghandour AA. Experimental and analytical investigation of CFRP flexural and shear strengthening efficiencies of RC beams. Constr Build Mater 2011;25:1419–29.